Toll-Like Receptor 4 Mediated Oxidized Low-Density Lipoprotein-Induced Foam Cell Formation in Vascular Smooth Muscle Cells

Zhongli Chen
Shanghai Jiao Tong University Medical School Affiliated Ruijin Hospital
Qiqi Xue
Shanghai Jiao Tong University Medical School Affiliated Ruijin Hospital
Lijuan Cao
Huanpu Branch Shanghai Ninth People's Hospital
Yanpin Wang
Shanghai Jiao Tong University Medical School Affiliated Ruijin Hospital
Yuanyuan Chen
Shanghai Jiao Tong University Medical School Affiliated Ruijin Hospital
Xiaojie Zhang
Zhongshan Hospital Fudan University
Fan Xiao
Shanghai Ninth people's hospital
Ying Yang
The Second People's Hospital of Yunnan
Melvin R. Hayden
University of Missouri
Liu Yan
Shanghai Ninth people's hospital
Ke Yang (ykk_ykkk@126.com)
Shanghai Jiao Tong University Medical School Affiliated Ruijin Hospital https://orcid.org/0000-0002-1870-1134

Original investigation

Keywords: Toll-like receptor 4, oxidized LDL, vascular smooth muscle cell, foam cell, atherosclerosis

Posted Date: June 18th, 2020

DOI: https://doi.org/10.21203/rs.3.rs-35206/v1

Abstract

Background: Oxidized low-density lipoprotein (oxLDL) induced a foam-cell like phenotype of the vascular smooth muscle cells (VSMCs), leading to the inflammatory responses incorporating Toll-like receptors (Tlrs)-mediated cellular alterations. We previously found that Tlr4 participated in inflammation response in VSMCs under oxLDL stimulation. However, the role of Tlr4 in foam-cell formation and underlying molecular pathways has not been comprehensively elucidated. This study aimed to investigate the role of Tlr4-mediated mechanisms in oxLDL induced foam-cell formation within VSMCs.

Methods: After incubated with different dose of oxLDL, the lipid, reactive oxygen species (ROS) accumulation and foam-cell phenotype of the VSMCs were detected. The alteration of Tlr family, ROS and lipid accumulation regulators including the Src kinase, Nox2, Nox4, Mnsod and sirtuins were measured. Then the Tlr4 was knock down and underlying cellular change and altered molecules were detected.

Results: We showed that oxLDL induced foam-cell like phenotype in VSMCs and led to lipid and ROS accumulation in a dose-dependent manner. OxLDL induced the strongest upregulation of Tlr4 in the Tlrs family and initiated change of Src activation, Nox2, Mnsod, sirt1 and sirt3 expression. The effect of oxLDL was abolished by Tlr4 knockdown. Furthermore, knocking down of Tlr4 reduced Src activation and led to restored Sirt1/Sirt3 expression. Moreover, inhibiting or knocking down the Src kinase diminished lipid accumulation in VSMCs under oxLDL treatment. And overexpression of Sirt1/3 relieved the oxLDL induced ROS accumulation and foam-cell phenotype in VSMCs.

Conclusions: These results demonstrated that Tlr4 is a critical regulator in oxLDL induced foam cell formation of VSMCs via mediating Src kinase as well as Sirt1 and Sirt3. Beyond the role of Tlr4 in inflammation response of VSMCs, we provide an integrated mechanism about TLR4 in VSMCs phenotype transition under oxLDL stimulation.

Background

Coronary artery disease (CAD) is a leading health burden contributing to high morbidity and mortality worldwide [1]. And atherosclerosis serves as the major cause driving the occlusion of coronary arteries and cardiovascular events [2]. During the process of atherosclerosis, mounting foam cells formation and necrosis invoked the inflammation storm, which aggravated instability of plaque and led to acute myocardial infraction [3, 4]. Previous studies showed that despite the well-established essential role of monocyte-derived macrophages, vascular smooth muscle cells (VSMCs) were equipped with macrophage features, constituting a substantial source of foam cells and inflammatory response in plaques [5, 6]. Basically, low density lipoprotein underwent oxidative modification beneath the vascular intimal, and could be ingested by VSMCs[7], which, promoted transition of VSMCs from the mature contractile state to the macrophage-like phenotype [8]. As a result, lipid accumulated in the VSMCs, and such VSMC-derived foam cells accelerated the progression of the atherosclerosis [9, 10]. Though a few scavenger receptors

participated in lipid uptake during foam cells formation, the specific mechanism contributing to lipid accumulation in VSMCs was still unclear. To acquire a better understanding of VSMCs alteration in atherosclerosis, it is necessary to clarify the mechanism underlying the lipid accumulation in VSMCs.

Along with the continuous formation and necrosis of the foam cells, regional inflammatory storm induced by excessive cytokines caused damage to the vessels [11]. OxLDL ingestion induced foam cells formation and soon afterwards, accelerated mitochondrial oxidative stress [12],[13], which led to accumulating reactive oxygen species (ROS) production [13].Taken together, these factors evoked inflammatory response signaling pathway in foam cells [14, 15]. In our previous studies, oxLDL activated pre-inflammatory signaling pathway and raised expression and secretion of inflammatory cytokines in VSMCs via Tlr4 [16]. Moreover, oxLDL promoted the bond of Tlr4 with Src kinase to induce lipid uptake and foam cell formation in macrophages [17]. Other studies also indicated that Tlr4 was implicated in foam cell formation in VSMCs. These results hint that Tlr4 might regulate lipid uptake process and subsequently contribute to foam cells formation in VSMCs. Nevertheless, such potential role of Tlr4 in the VSMCs has not been explored.

Additionally, excessive production of reactive oxygen species (ROS) was widely observed in atherosclerosis. Although it has been well-established that the broken oxidative homeostasis could promote the vascular inflammation response, the relationship between oxidative stress and foam cell formation in VSMCs has not been elucidated. Several previous studies showed that Tlr4 mediated ROS accumulation via regulating Nox2 [18]. The pivotal role of emerging sirtuins family in maintaining the balance of the ROS metabolism has also been increasingly reported [19]. However, whether they were involved in oxLDL-TLR4 induced VSMCs inflammation and ROS accumulation remain obscure.

In this study, we hypothesized that Tlr4 mediated oxLDL-induced foam cell formation via regulating lipid accumulation and ROS production in VSMCs. Based on cellular and molecular research, we aimed to clarify the mechanism underlying the ROS and lipid accumulation induced by oxLDL in VSMCs, thus deepening the insights about the formation of foam cell-like VSMCs during atherosclerosis.

Methods

Reagents and Antibodies

Fetal bovine serum (Cat#16000), advanced DMEM/F-12 (Cat#12634010) and antibiotic-antimycotic (Cat#15240096) were obtained from Gibco (CA, USA). OxLDL (Cat#L34357), Nile Red (Cat#N1142), Image-IT™ LIVE Green Reactive Oxygen Species Detection Kit (Cat#I36007), MitoSOX™ Red Mitochondrial Superoxide Indicator (Cat#M36008), DAPI (Cat#D1306), TRIzol™ Reagent (Cat#15596026), Goat anti-Rabbit secondary antibody conjunction with Alexa Fluor Plus 555 (Cat#A-21429), Goat anti-Mouse secondary antibody conjunction with Alexa Fluor Plus 488 (Cat#A-11001) and Lipofectamine™ RNAi MAX transfection reagent (Cat#13778150) were purchased from Invitrogen (CA, USA). Tlr4 siRNA (Cat#sc-40261), Src siRNA (Cat#sc-29859) and negative control siRNA (Cat#sc-37007) were bought from Santa

Cruz (TX, USA). Let-blank (Cat#GCNL), Let-Sirt1 (+) (Cat#GCD0161581) and Let-sirt3 (+) (Cat#GCD0201555) were acquired from Shanghai Genechem (Shanghai, China). Premix ex taq™ DNA polymerase (Cat#RR039A) and primeScript™ 1st strand cDNA synthesis kit (Cat#6110A) were collected from TaKaRa (Tokyo, Japan). HDL and LDL/VLDL cholesterol assay kit (Cat#ab65390), H&E stainning kit (Cat#ab245880), BCA protein assay kit (Cat#ab102536), PP2 (Cat#ab120308), PP3 (Cat#ab120617) and the primary antibody of Myh11 (Cat#ab53219), αSma (Cat#ab52218), Mac2 (Cat#ab2785), Cd68 (Cat#ab31630), Nox2 (Cat#ab80508), Nox4 (Cat#ab14544) and Sirt4 (Cat#ab124521) were purchased from Abcam (MA, USA). Additionally, primary antibody of β-actin (Cat#3700), p-Src Y418 (Cat#6943), t-Src (Cat#2123), Mnsod (Cat#13141), Sirt1 (Cat#2314), Sirt2 (Cat#12650), Sirt3 (Cat#5490), Sirt5 (Cat#8782), Sirt6 (Cat#12486), Sirt7 (Cat#5360) and tlr4 (Cat#14358) as well as the second antibody-conjunction HRP anti-mouse/rabbit (Cat#7076/ Cat#7074) were gained from CST (MA, USA).

Primary Smooth Muscle Cells Culture

Wild-type (C57BL/6) mice were purchased from Model Animal Research Center of Nanjing University (Nanjing, China) and were euthanized at 4 weeks old. To obtain the primary smooth muscle cells, the aortas of the mice were dissected and the adventitia was removed. The aortic explants were cultured after mechanical dissection and twice washes in PBS. The explant-derived VSMCs were cultured at 37℃,5% CO_2 in F12: DMEM (1:1) medium with 20% fetal bovine serum and 1% antibiotic-antimycotic. The animal experiment protocol complied with the Animal Management Rules of the Chinese Ministry of Health (Document No. 55, 2001) and was approved by the Animal Care Committee of Shanghai Jiaotong University.

Assessment of Intracellular Lipids

VSMCs were cultured in 6-well plates and incubated with oxLDL for 72 hours. Afterward, the VSMCs were washed by PBS for twice followed by 15-minute 4% paraformaldehyde/PBS fixation and then were stained by 100 ng/mL Nile Red for intracellular lipids detection [20]. All cell samples were observed and photographed microscopically (ZEISS LSM 800, Zeiss Microsystems). 5 fields of view were randomly acquired and representative images were shown. Intracellular lipids were quantified by HDL and LDL/VLDL Cholesterol Assay Kit. Quantifications of total lipoprotein was conducted according to description in the manufacturer's protocols and demonstrated as relative values-to-total protein ratio (n=3).

Intracellular Reactive Oxygen Species Assay

Cellular ROS protection was detected by carboxy-H2DCFDA kit. Based on the kit instruction, 25 μM carboxy-H2DCFDA working solution was used to label VSMCs for 30 minutes at 37°C in dark. Afterward, cells were gently washed in warm HBSS/Ca/Mg and incubated with Hoechst 33342 for another 5 minutes. After 3 times washes, the ROS signals were observed via a fluorescent microscope. 5 fields of view were randomly acquired and representative images were showed.

Assessment of intracellular Mitochondrial Superoxide

After incubation with oxLDL, VSMCs were gently washed by warm Hanks buffer. The mitochondrial superoxide was detected using the MitoSOX™ Red indicator. According to the manufacturer's recommendation, the MitoSOX™ reagent was diluted into a working concentration and added to the 6 well plate covering the VSMCs. After 10 minute-incubation at 37 ℃ in dark, the cells were washed by Hanks buffer for three times. Image were obtained by fluorescence microscope using a green excitation light. 5 fields of view were randomly acquired and representative images were showed.

Quantitative Real-time RT-PCR

Total RNA was extracted by Trizol reagent, and 5 ug of total RNA undergone the reverse-transcription. Polymerase chain reactions (PCR) were carried out using Power SYBR Green PCR Master Mix (Applied BioSystems, CA, USA) according to the manufacturer's recommendation in a StepOne System (Applied BioSystems, CA, USA). Primers for the promoter sequences were listed in (**Table 1**). Gene expression were normalized with β-actin as the reference gene. StepOne software v2.1 (Applied BioSystems) was used for data analysis.

Table 1
The primer has been used for Realtime-PCR.

Gene	Forward primer	Reverse primer	Products size (bP)
Myh11	5‘-AAG CTG CGG CTA GAG GTC A-3’	5‘-CCC TCC CTT TGA TGG CTG AG-3’	238
αSma	5‘-GTC CCA GAC ATC AGG GAG TAA-3’	5‘-TCG GAT ACT TCA GCG TCA GGA-3’	102
Mac2	5‘-AGG AGA GGG AAT GAT GTT GCC-3’	5‘-GGT TTG CCA CTC TCA AAG GG-3’	143
Cd68	5‘-TTG GGA ACT ACA CAC GTG GGC-3’	5‘-CGG ATT TGA ATT TGG GCT TG-3’	67
Tlr1	5‘-CAA TGT GGA AAC AAC GTG GA-3’	5‘-TGT AAC TTT GGG GGA AGC TG-3’	200
Tlr2	5‘-AAG AGG AAG CCC AAG AAA GC-3’	5‘-CGA TGG AAT CGA TGA TGT TG-3’	199
Tlr3	5‘-CAC AGG CTG AGC AGT TTG AA-3’	5‘-TTT CGG CTT CTT TTG ATG CT-3’	190
Tlr4	5‘-ACC TGG CTG GTT TAC ACG TC-3’	5‘-CTG CCA GAG ACA TTG CAG AA-3’	201
Tlr5	5‘-AAG TTC CGG GGA ATC TGT TT-3’	5‘-GCA TAG CCT GAG CCT GTT TC-3’	201
Tlr6	5‘-TTC CCA ATA CCA CCG TTC TC-3’	5‘-CTA TGT GCT GGA GGG TCA CA-3’	201
Tlr7	5‘-AAT CCA CAG GCT CAC CCA TA-3’	5‘-CAG GTA CCA AGG GAT GTC CT-3’	142
Tlr8	5‘-GAC ATG GCC CCT AAT TTC CT-3’	5‘-GAC CCA GAA GTC CTC ATG GA-3’	195
Tlr9	5‘-ACT GAG CAC CCC TGC TTC TA-3’	5‘-AGA TTA GTC AGC GGC AGG AA-3’	198
Tlr11	5‘-CCA GGA CTG CAC CTT TTG G-3’	5‘-GTG ACA CTG GTT GTA CGC AAT-3’	185
Tlr12	5‘-TTG GAA GTT GTA CCT CGG ACT-3’	5‘-GAA GTT GGG TAA GGT GCA GAC-3’	130
Tlr13	5‘-GTT GTA ACC TGG ATG CCT AAG AC-3’	5‘-GGC CTC TGT CAA GTT GGT GA-3’	198
β-actin	5‘-GAC AGG ATG CAG AAG GAG A-3’	5‘-CCA CAT CTG CTG GAA GGT GG-3’	138

Western Blot

VSMCs were lysed in Western & IP Cell lysate on ice for 15 min. The total protein was collected after centrifugation. Protein concentration was measured using a BCA-protein assay kit. Equal quantification of protein (20 μg) was applied in a 15% SDS-polyacrylamide gel and transferred to polyvinylidene fluoride (PVDF) membranes. The membranes were blocked by 5% milk for 1 hours at room temperature and then incubated with the primary antibody overnight at 4°C. After 3 times washed in TBS buffer, the membrane was incubated with horseradish peroxidase (HRP)-conjugated secondary antibodies at room temperature for 2 hours. Finally, Images were captured in a Tanon-5500 chemiluminescent imaging system (Tanon Science and Technology Co., Ltd., Shanghai, China) and quantified by ImageJ software (Bio-Rad, Hercules, CA, USA).

Oligonucleotide Transfection

RNA interference was conducted using the Oligo-fectamine reagent (Invitrogen). A non-targeting sequence was used as control siRNA. And cultured VSMCs were transfected with the siRNA and control according to the instruction. Cells had 60%-70% confluency at the day of transfection. After transfecting for 48 hours, the knockdown efficiency was tested by western-blot.

Pretreatment with PP2 and PP3

PP2 (10 μmol/L) and PP3 (10 μmol/L) were respectively added to VSMCs and incubated for 30 min before oxLDL stimulation. PP3 served as the negative control for PP2.

Sirt1 and Sirt3 Overexpression Lentivirus production and Transfection

The Sirt1 and Sirt3 overexpression was completed using recombinant lentivirus vectors containing the overexpression plasmid of the corresponding gene. Empty vector lentivirus was also transfected as control. Cells were infected with lentivirus for 72 hours followed by a RT-PCR for efficiency determination.

Statistical Analysis

Values were showed as mean with standard deviation (SD). Paired samples were compared using Student’s paired t-test. One-way ANOVA followed by Friedman’s post-test was used for multiple group comparisons. A two-sided p value less than 0.05 was considered statistically significant. Data were analyzed and plotted using the Graphpad Prism Version 7.0.

Results

OxLDL induced dose-dependent lipid accumulation, oxidative stress and foam cell formation in vascular smooth muscle cells.

After stimulated by gradient dose (12.5, 25 and 50 μg/mL) of oxLDL for 48 hours, lipid accumulation, cellular ROS accumulation, mitochondrial superoxide generation and foam cells formation was

examined. The Nile Red staining and lipoprotein quantification showed that oxLDL induced lipid accumulation in VSMCs in a dose-dependent manner **(Figure 1.A)**. The DCFH-DA and MitoSOX served as detectors for labeling cellular ROS and mitochondrial superoxide generation respectively. Similar to the oxLDL-induced lipid accumulation, higher concentration of oxLDL triggered severe oxidative stress within cell and mitochondrial **(Figure 1.B and C)**.

Moreover, after oxLDL stimulation, the expression of αSma and Myh11, the contractile phenotype-specific mRNA and protein, was down-regulated, while the foam cells' phenotype markers, Cd68 and Mac2, were significantly upregulated **(Figure 1. D-F)**.

OxLDL mediated significant upregulation of Tlr4 along with expression/ activation of lipid metabolism and oxidative stress regulators.

To explore the overall change of the Tlrs family under the oxLDL stimulation in VSMCs, we further measured mRNA levels of the Tlrs in VSMCs after 48 hours incubation with 50 μg/mL of oxLDL to figure out which members of the Tlrs experienced drastic change. Remarkably, under oxLDL treatment, expression of Tlr4 increased more significant than any other Tlrs among Tlr1-Tlr13 (**Figure 2.A**), with over 1.5-fold expression than the control. In our previous study had explored the protein level of Tlr4 increased with oxLDL stimulation in VSMCs[16].

Based on our previous observations in macrophages [17], activation of Src in VSMCs was measured after gradient dose (12.5, 25 and 50 μg/mL) of oxLDL stimulation for 1 hour. In line with the macrophage, we found that the phosphorylation site of Src (418-Tyr) was obviously activated in VSMCs. But different from the result of macrophages, Src did not show a dose-dependent effect in such activation and the extend of activation was comparable across different oxLDL concentration-treated group (upper of **Figure 2.B**). Meanwhile, the expression of the ROS elimination-relevant gene Mnsod as well as Nox2 and Nox4, which are responsible for ROS generation were examined. Only the highest dose (50 μg/mL) of oxLDL resulted in significant elevation of Nox2 and remarkable decreased Mnsod, whereas the significant change of Nox4 expression was not observed. (bottom of **Figure 2.B**). Finally, the alteration of the oxidative balance maintainer, sirtuins family, were also explored. It is interesting to note that only expression of Sirt1 and Sirt3 were remarkably downregulated while no significant effect was observed in terms of other members of sirtuins family (**Figure 2.C**).

Tlr4 mediated oxLDL-induced lipid accumulation, oxidative stress and foam cell formation in VSMCs

To investigate the role of Tlr4 in oxLDL-induced pathophysiological change and its relation with those altered regulators in VSMCs, Tlr4 was knockdown to further elaborate subsequent cellular phenomenon and molecular pathway. Tlr4 were significantly knockdown by targeted siRNA and negative control siRNA (NC) was also transfected to serve as negative control (**Figure 3.A**). After 50μg/mL of oxLDL stimulation for 48 hours, lipid accumulation, ROS and mitochondrial superoxide were still sharply promoted in NC group. By contrast, these alterations were ameliorated in Tlr4- knockdown VSMCs (**Figure 3.B-D**). More importantly, although oxLDL still led to significant decrease of VSMCs contractile phenotype marker

(Myh11 and αSma) and elevated foam cells marker (Mac2 and Cd68) in NC VSMCs, TLR4 knockdown had interrupted most of these alterations, indicating that TLR4, at least partly mediated the oxLDL induced lipid and ROS accumulation and contribute to foam cell formation (**Figure 3.E and F**).

Tlr4-Src kinase regulated lipid accumulation and cellular phenotype transition in VSMCs

Notably, after knocking down the Tlr4 in VSMCs, the activation in Tyr-418 phosphorylation site of Src kinase were deprived to a great extent, compared with the NC group, after 1-hour oxLDL treatment (**Figure 4.A and B**). Such effect indicated that Tlr4 regulated Src kinase activation under oxLDL stimulation. And we further hypothesized that Src kinase might be downstream executor of TLR4 to impact lipid uptake in VSMCs. To illuminate this hypothesis, either the expression or the activation of Src were disturbed by siRNA or PP2 respectively, and then the change of intracellular lipid concentration and cell phenotype markers were determined following oxLDL treatment. The efficiency of siRNA knockdown Src was tested with western-blot (**Figure 4.C and D**). Compared with untreated group, higher intercellular lipid levels were observed in oxLDL-treated groups, but Src knockdown or activation-blocked groups showed relative less lipid accumulation than NC or PP3 groups (**Figure 4.E**). Furthermore, knocking down the expression or blocking the activation of Src significantly postponed the loss of VSMCs contractile markers loss and of foam cell phenotype gaining, which were induced by oxLDL (**Figure 4.F and G**).

Tlr4 mediated Sirt1/Sirt3 alteration which regulated oxLDL-induced oxidative stress and foam cell formation in VSMCs

Interestingly, we also observed that when Tlr4 in VSMCs was knocked down, the expression of Sirt1 and Sirt3 restored compared with the NC group after 48-hours oxLDL treatment accompanied by reduced Nox2 and elevated Mnsod expression, implying that Tlr4 contributed to Sirt1 and Sirt3 downregulation under oxLDL stimulation (**Figure 5.A-B)**.

To investigate whether Sirt1 and Sirt3 could antagonize oxLDL-induced ROS accumulation, mitochondrial superoxide and foam cell formation in VSMCs, recombined lentivirus of Sirt1 [Let-Sirt1(+)] or Sirt3 [Let-Sirt3(+)] overexpression were transfected SMCs. The Let-Sirt1(+) or Let-Sirt3(+) significantly increased the expression of Sirt1 and Sirt3 respectively without mutual interference **(Figure 5.C and D)**. Compared with untreated group, addition of oxLDL caused significantly ROS and mitochondrial superoxide accumulation in VSMCs. However, compared with NC group, Sirt1 and Sirt3 overexpression groups displayed alleviated oxidative stress **(Figure 5.E and F)**. Additionally, though oxLDL led to significantly elevated Nox2 and decreased Mnsod, Sirt1 or Sirt3 overexpression almost reversed such impact on these genes **(upper, Figure 5.G and H)**. Moreover, increased expression of Sirt1 or Sirt3 also relive the oxLDL-induced VSMCs contractile phenotype marker (Myh11 and αSma) loss and foam cells marker (Mac2 and Cd68) acquisition, though they were still significantly altered compared with the untreated group, which implied that Sirt1 and Sirt3 partly assist in VSMCs phenotype rebalancing under oxLDL stimulation (**bottom, Figure 5.G and H**).

Discussion

In this study, we demonstrated that oxLDL induced the transition of VSMCs to foam cells by promoting lipid accumulation and ROS production via raising the expression of a key linking molecular-Tlr4. Furthermore, oxLDL-induced lipid and ROS accumulation were at least partly attributed to Tlr4-regulated Src activation and Sirt1 and Sirt3 upregulation, which also contributed to foam cells formation. Our findings unraveled a crucial role of Tlr4 in oxLDL-induced foam cell formation in VSMCs.

The toll-like receptors family constitute important members of pattern recognition receptors (PRRs), which identify special ligand of receptor to evoke pathogen-associated molecular patterns (PAMPs) [21–23]. These innate immune responses are commonly activated in innate immune cells. Likewise, as a chronic inflammation process, atherosclerosis was closely bound with the continuous innate immune response triggered by activation of PPRs [24]. Basically, oxLDL is a principle component of endogenous lipid ligand that causes endothelial cell injury, accumulates in macrophage and VSMCs and induces a cellular inflammation response [25, 26]. Tlrs were reported to participate in oxLDL induced inflammation response[27–29], but an integrated expression feature of Tlrs family in VSMCs under oxLDL stimulation remained unelaborated. In our present study, we found that oxLDL raised the expression of Tlr4 more significantly, which was over 1.5-fold than other Tlrs in VSMCs. Such observations suggested that among the Tlrs family, Tlr4 might serve as major participant in oxLDL induced alterations of VSMCs.

Foam cell phenotype and inflammation response are two major interrelated alterations in VSMCs that exacerbated the progression of atherosclerosis [6]. Our work provided evidence for the role of Tlr4 throughout the oxLDL-induced change in VSMCs. Previously, we certificated that Tlr4 was a crucial inflammation regulator in oxLDL-induced inflammatory cytokine expression/secretion as well as p38 and NFκB activation [16]. Herein, we also detected the role of Tlr4 in the prior foam cell formation in the VSMCs. In this study, besides gradient upregulation of Tlr4, we evidenced that knocking down Tlr4 could reverse oxLDL-induced phenotype change, which was characterized by emerging foam cells phenotype and weakened contractile phenotype in VSMCs. Taken together, we found that Tlr4 not only played a crucial role in oxLDL-induced inflammatory response, but also mediated oxLDL-induced foam cells formation in VSMCs (Fig. 6).

Foam cell formation, characterized by accumulation of intracellular lipids and occurrence of inflammatory phenotype, is a hallmark in progression of atherosclerosis [30]. Lipid loading in VSMCs activated multiple pro-inflammatory genes, suppressed expression of VSMC marker genes, and led to the phenotype switching as well as inflammatory cytokines secretion [31]. Herein, we found that oxLDL evoked lipid accumulation in VSMCs, and knocking down the Tlr4 inhibited such lipid uptake in VSMCs, implying that Tlr4 mediated oxLDL-induced lipid accumulation and promoted subsequent foam cells formation. In a previous studies we were able to demonstrate that Tlr4 directly participated in oxLDL-induced lipid uptake in macrophages by regulating Src kinase [17], indicating that Tlr4 was not only an innate immune receptor in inflammatory response, but also a mediator for lipid accumulation. Although little was known about the role of Tlr4 in lipid accumulation of VSMCs, herein we evidenced that Tlr4-Src

signaling contributed to lipid accumulation of VSMCs and further demonstrated that the foam cell phenotype could be partly reversed after interfering Tlr4 or Src. These observations suggest that TLR4-Src pathway might be a common regulation mechanism of oxLDL-induced lipid accumulation and foam cell formation in atherosclerosis (Fig. 6). Actually, it might be reasonable that Src could serve as a downstream molecule contributing to the lipid loading in VSMCs. Firstly, activation of Src may mediate the rearrangement of the cytoskeleton, which is a major cellular alteration underling endocytosis [32]. Additionally, Src signaling activates c-Jun N-terminal kinase and enhances the trans-activity of c-Jun in response to LPS, thus triggering the expression of inflammation markers [33, 34]. Therefore, Src is likely to alter the lipid accumulation and inflammation response in the VSMCs.

ROS was a well-known mediator that exerts severe intracellular oxidative stress and prompts inflammatory response, structural reorganization, and even cell phenotype transition [35, 36]. In our present study, we found that oxLDL promoted intracellular ROS and mitochondrial superoxide accumulation. In terms of this remarkable cytological event, we explored the remarkable cytological event from dialectical aspects, including both the ROS generation through Nox2 and Noxr4 and the ROS elimination via Mnsod, which constitute the balance of “in” and “out” on a “tank”. We found that oxLDL led to overflow of ROS production through accelerating speed of “in” (increasing Nox2 expression but not Nox4) and decelerating speed of “out” (decreasing Mnsod expression) in VSMCs. Along with the reversed phenotype alteration of VSMCs, knockdown of Tlr4 also inhibited ROS and mitochondrial superoxide production, reduced Nox2 expression and increased Mnsod expression, suggesting that the ROS production speed of “in” or “out” were regulated by Tlr4. These results indicated that Tlr4 mediated oxLDL-induced ROS accumulation through regulating the balance of ROS homeostasis, which might be another potential mechanism of Tlr4 during foam cells formation in VSMCs.

Since previous studies showed that Sirtuin family members were located in nuclear and mitochondrial organelles, maintaining redox homeostasis via regulating the oxidative stress-associate genes [19], we also examined whether the Sirtuin family participate in the Tlr4-mediated oxidative alteration during foam cell formation of VSMCs. We found that amid the Sirtuins family, Sirt1 and Sirt3 were downregulated most significantly after oxLDL stimulation. As previous publications revealed that Sirt1 and Sirt3 were capable of suppressing ROS accumulation through inhibiting the activities of Nox and activating the Mnsod in aging and carcinogenesis [37–39], we hypothesized that Sirt1 and Sirt3 may also serve as upstream molecules to regulate Nox2 and Mnsod expression in VSMCs during atherosclerosis. In line with these findings, we observed that overexpression of Sirt1 and Sirt3 upregulated Mnsod but downregulated Nox2 under oxLDL treatment. Furthermore, raising the expression of Sirt1 and Sirt3 inhibited production of ROS and foam cells phenotype in VSMCs. These results illustrated that Sirt1 and Sirt3 participated in ROS accumulation and foam cells formation via regulating Nox2 and Mnsod expression and regulating Sirt1 and Sirt3 might alleviate the oxidative stress and foam-cell formation in VSMCs. More importantly, when considering reversed expression of Sirt1 and Sirt3 after knockdown of Tlr4, we concluded that oxLDL promoted ROS accumulation via Tlr4-Sirt1/3 signaling pathway, thus inducing the foam-cell phenotype of VSMCs (Fig. 6).

Conclusions

Our study demonstrated that Tlr4 is a critical regulator in oxLDL induced foam cell formation of VSMCs via mediating Src kinase as well as Sirt1 and Sirt3. Beyond the role of Tlr4 in the inflammation response of VSMCs, we provided an integrated mechanism about Tlr4 in VSMCs phenotype transition under oxLDL stimulation.

Abbreviations

oxLDL: Oxidized low-density lipoprotein

VSMCs: vascular smooth muscle cells

Tlrs: Toll-like receptors

ROS: Reactive oxygen species

CAD: Coronary artery disease

PVDF: Polyvinylidene fluoride

HRP: Horseradish peroxidase

SD: Standard deviation

PRRs: Pattern recognition receptors

PAMPs: Pathogen-associated molecular patterns

Sirt1: Sirtuin 1

Sirt3: Sirtuin 3

Declarations

Ethics approval and consent to participate

The animal experiment protocol complied with the Animal Management Rules of the Chinese Ministry of Health (Document No. 55, 2001) and was approved by the Animal Care Committee of Shanghai Jiaotong University

Consent for publication

Not applicable

Availability of data and materials

The datasets used and/or analyzed during the current study are available from the corresponding author on reasonable request.

Competing interests

The authors declare that they have no competing interests.

Funding

This work was supported by grants from the Natural Science Foundation of China (81760734, 81770384 and 31660313), the Natural Science Foundation of Yunnan Province (No. 2017FA048), the fund of Diabetic Innovation Team (2019HC002) and Endocrine Clinical Medical Center of Yunnan Province (No. ZX2019-02-02). The fund of medical leader in Yunnan Province (No. L-201609).

Authors' contributions

Study conception and design: Yang. K. and Liu. Y.

Acquisition and analysis of data: Chen. ZL., Xue. QQ., Cao. LJ., Wang. YP., Chen. YY., Zhang. XJ., Xiao. F. and Yang. Y.

Drafting a significant portion of the manuscript or figures: Chen. ZL., Hayden, MR., Yang. K. and Liu. Y.

All authors read and approved the final manuscript.

Acknowledgements

We would like to thank Dr. Ying Huang and her associates in the core facility unit (School of Medicine, Shanghai Jiao Tong University) for their professional support in imaging capture and processing.

References

1. Boudoulas KD, Triposciadis F, Geleris P, Boudoulas H. Coronary Atherosclerosis: Pathophysiologic Basis for Diagnosis and Management. Prog Cardiovasc Dis. 2016;58(6):676–92.
2. Libby P, Buring JE, Badimon L, Hansson GK, Deanfield J, Bittencourt MS, Tokgözoğlu L. Lewis EF: **Atherosclerosis**. Nature reviews Disease primers. 2019;5(1):56.
3. Chistiakov DA, Melnichenko AA, Myasoedova VA, Grechko AV, Orekhov AN. Mechanisms of foam cell formation in atherosclerosis. J Mol Med (Berl). 2017;95(11):1153–65.
4. Maguire EM, Pearce SWA, Xiao Q. Foam cell formation: A new target for fighting atherosclerosis and cardiovascular disease. Vascul Pharmacol. 2019;112:54–71.
5. Basatemur GL, Jørgensen HF, Clarke MCH, Bennett MR, Mallat Z. Vascular smooth muscle cells in atherosclerosis. Nature reviews Cardiology. 2019;16(12):727–44.

6. Bennett MR, Sinha S, Owens GK. Vascular smooth muscle cells in atherosclerosis. Circulation research. 2016;118(4):692–702.
7. Hayden MR, Sowers JR, DeMarco VG. **ULTRASTRUCTURE STUDY OF THE TRANSGENIC REN2 RAT AORTA–PART 2: MEDIA, EXTERNAL ELASTIC LAMINA, AND ADVENTITIA**. *BMR* 2019:112.
8. Pi H, Wang Z, Liu M, Deng P, Yu Z, Zhou Z, Gao F. SCD1 activation impedes foam cell formation by inducing lipophagy in oxLDL-treated human vascular smooth muscle cells. J Cell Mol Med. 2019;23(8):5259–69.
9. Allahverdian S, Chaabane C, Boukais K, Francis GA, Bochaton-Piallat ML. Smooth muscle cell fate and plasticity in atherosclerosis. Cardiovasc Res. 2018;114(4):540–50.
10. Di Pietro N, Formoso G, Pandolfi A. Physiology and pathophysiology of oxLDL uptake by vascular wall cells in atherosclerosis. Vascul Pharmacol. 2016;84:1–7.
11. Wang F, Zhang Z, Fang A, Jin Q, Fang D, Liu Y, Wu J, Tan X, Wei Y, Jiang C, et al. Macrophage Foam Cell-Targeting Immunization Attenuates Atherosclerosis. Front Immunol. 2018;9:3127.
12. Chistiakov DA, Bobryshev YV, Orekhov AN. Macrophage-mediated cholesterol handling in atherosclerosis. J Cell Mol Med. 2016;20(1):17–28.
13. Kattoor AJ, Pothineni NVK, Palagiri D, Mehta JL. Oxidative Stress in Atherosclerosis. Curr Atheroscler Rep. 2017;19(11):42.
14. Kotla S, Singh NK, Rao GN. ROS via BTK-p300-STAT1-PPARgamma signaling activation mediates cholesterol crystals-induced CD36 expression and foam cell formation. Redox Biol. 2017;11:350–64.
15. Fan J, Liu L, Liu Q, Cui Y, Yao B, Zhang M, Gao Y, Fu Y, Dai H, Pan J, et al. CKIP-1 limits foam cell formation and inhibits atherosclerosis by promoting degradation of Oct-1 by REGgamma. Nat Commun. 2019;10(1):425.
16. Yang K, Zhang XJ, Cao LJ, Liu XH, Liu ZH, Wang XQ, Chen QJ, Lu L, Shen WF, Liu Y. Toll-like receptor 4 mediates inflammatory cytokine secretion in smooth muscle cells induced by oxidized low-density lipoprotein. PLoS One. 2014;9(4):e95935.
17. Yang K, Wang X, Liu Z, Lu L, Mao J, Meng H, Wang Y, Hu Y, Zeng Y, Zhang X, et al. Oxidized low-density lipoprotein promotes macrophage lipid accumulation via the toll-like receptor 4-Src pathway. Circulation journal: official journal of the Japanese Circulation Society. 2015;79(11):2509–16.
18. Singh A, Singh V, Tiwari RL, Chandra T, Kumar A, Dikshit M, Barthwal MK. The IRAK-ERK-p67phox-Nox-2 axis mediates TLR4, 2-induced ROS production for IL-1beta transcription and processing in monocytes. Cell Mol Immunol. 2016;13(6):745–63.
19. Singh CK, Chhabra G, Ndiaye MA, Garcia-Peterson LM, Mack NJ, Ahmad N. The Role of Sirtuins in Antioxidant and Redox Signaling. Antioxid Redox Signal. 2018;28(8):643–61.
20. Escorcia W, Ruter DL, Nhan J, Curran SP. **Quantification of Lipid Abundance and Evaluation of Lipid Distribution in Caenorhabditis elegans by Nile Red and Oil Red O Staining**. *J Vis Exp* 2018(133).
21. Bauer S, Muller T, Hamm S. Pattern recognition by Toll-like receptors. Adv Exp Med Biol. 2009;653:15–34.

22. Murillo LS, Morre SA, Pena AS. Toll-like receptors and NOD/CARD proteins: pattern recognition receptors are key elements in the regulation of immune response. Drugs of today. 2003;39(6):415–38.
23. Huysamen C, Brown GD. The fungal pattern recognition receptor, Dectin-1, and the associated cluster of C-type lectin-like receptors. FEMS Microbiol Lett. 2009;290(2):121–8.
24. Li B, Xia Y, Hu B. **Infection and atherosclerosis: TLR-dependent pathways**. *Cellular and molecular life sciences: CMLS* 2020:1–19.
25. Steinberg D. The LDL modification hypothesis of atherogenesis: an update. Journal of lipid research. 2009;50(**Suppl**(Suppl):376–81.
26. Miller YI, Shyy JY. Context-Dependent Role of Oxidized Lipids and Lipoproteins in Inflammation. Trends Endocrinol Metab. 2017;28(2):143–52.
27. Bhaskar S, Helen A. Quercetin modulates toll-like receptor-mediated protein kinase signaling pathways in oxLDL-challenged human PBMCs and regulates TLR-activated atherosclerotic inflammation in hypercholesterolemic rats. Mol Cell Biochem. 2016;423(1–2):53–65.
28. Yang K, Liu X, Liu Y, Wang X, Cao L, Zhang X, Xu C, Shen W, Zhou T. DC-SIGN and Toll-like receptor 4 mediate oxidized low-density lipoprotein-induced inflammatory responses in macrophages. Sci Rep. 2017;7(1):3296.
29. Li Y, Shen S, Ding S, Wang L. Toll-like receptor 2 downregulates the cholesterol efflux by activating the nuclear factor-kappaB pathway in macrophages and may be a potential therapeutic target for the prevention of atherosclerosis. Exp Ther Med. 2018;15(1):198–204.
30. Bäck M, Yurdagul A Jr, Tabas I, Öörni K, Kovanen PT. Inflammation and its resolution in atherosclerosis: mediators and therapeutic opportunities. Nature reviews Cardiology. 2019;16(7):389–406.
31. Allahverdian S, Pannu PS, Francis GA. Contribution of monocyte-derived macrophages and smooth muscle cells to arterial foam cell formation. Cardiovasc Res. 2012;95(2):165–72.
32. Davidson L, Pawson AJ, Millar RP, Maudsley S. Cytoskeletal reorganization dependence of signaling by the gonadotropin-releasing hormone receptor. J Biol Chem. 2004;279(3):1980–93.
33. Kasahara K, Nakayama Y, Sato I, Ikeda K, Hoshino M, Endo T, Yamaguchi N. Role of Src-family kinases in formation and trafficking of macropinosomes. Journal of cellular physiology. 2007;211(1):220–32.
34. Smolinska MJ, Horwood NJ, Page TH, Smallie T, Foxwell BM. Chemical inhibition of Src family kinases affects major LPS-activated pathways in primary human macrophages. Molecular immunology. 2008;45(4):990–1000.
35. Moldogazieva NT, Mokhosoev IM, Mel'nikova TI, Porozov YB, Terentiev AA. Oxidative Stress and Advanced Lipoxidation and Glycation End Products (ALEs and AGEs) in Aging and Age-Related Diseases. Oxid Med Cell Longev. 2019;2019:3085756.
36. Marchio P, Guerra-Ojeda S, Vila JM, Aldasoro M, Victor VM, Mauricio MD. Targeting Early Atherosclerosis: A Focus on Oxidative Stress and Inflammation. Oxid Med Cell Longev.

2019;2019:8563845.

37. Tao R, Vassilopoulos A, Parisiadou L, Yan Y, Gius D. Regulation of MnSOD enzymatic activity by Sirt3 connects the mitochondrial acetylome signaling networks to aging and carcinogenesis. Antioxid Redox Signal. 2014;20(10):1646–54.
38. Salminen A, Kaarniranta K, Kauppinen A. Crosstalk between Oxidative Stress and SIRT1: Impact on the Aging Process. Int J Mol Sci. 2013;14(2):3834–59.
39. Chen Y, Zhang J, Lin Y, Lei Q, Guan KL, Zhao S, Xiong Y. Tumour suppressor SIRT3 deacetylates and activates manganese superoxide dismutase to scavenge ROS. EMBO Rep. 2011;12(6):534–41.

Figures

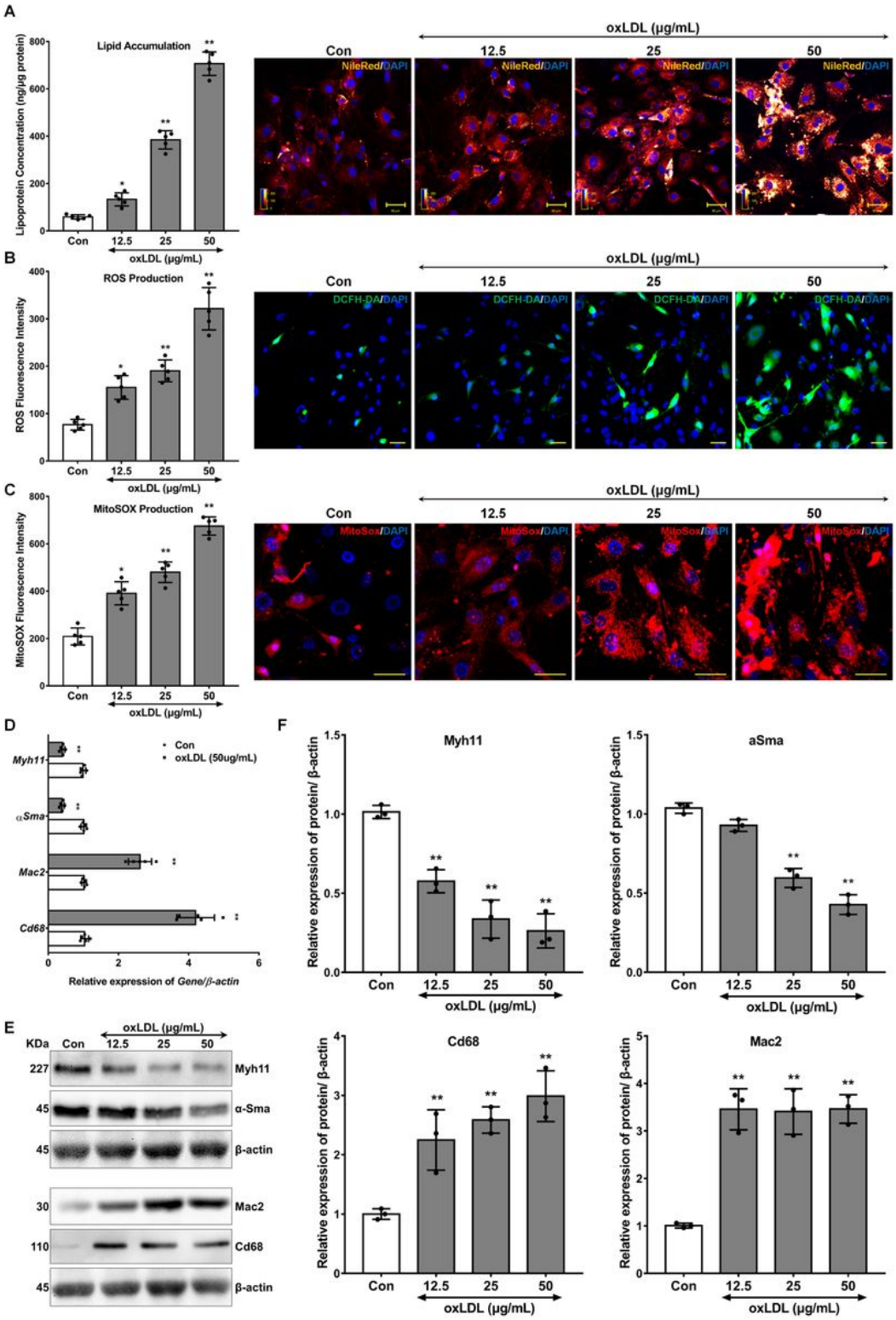

Figure 1

Oxidized low-density lipoprotein (oxLDL) induced lipid accumulation, reactive oxygen species (ROS), mitochondrial superoxide production and foam cells formation in vascular smooth muscle cells (VSMCs). After treating with doses of oxLDL (12.5, 25 and 50 μg) for 48 hours, the lipid accumulation, ROS and mitochondrial superoxide in VSMCs were measured, with the untreated group serving as control reference (Con). A. Nile Red (Orange) was used to stain the lipid and the concentration of lipoprotein was

measured. B. DCFH-DA (Green) labeled ROS and density of ROS production were detected. C. MitoSOX (Red) labeled mitochondrial superoxide and level of superoxide were calculated. (n=5 per group, results are expressed as Mean±SD; compared with the Con group by repeated-measures ANOVA followed by the Dunnett multiple comparisons test, *P<0.05, **P<0.01). After oxLDL stimulation, the mRNA or protein expression of genes (Myh11 and αSma as VSMCs contractile phenotype marker, Mac2 and Cd68 as foam cells marker) had been detected by real-time PCR or western-blot in VSMCs. Untreated group served as control (Con), and β-actin served as internal reference gene to normalize protein expression. All of the real-time PCR result were calculated with 2-ΔΔCT method, the western-blot results were calculated using grayscale value. D. mRNA levels of Myh11, αSma, Mac2 and Cd68 were measured by real-time PCR. (n=5 per group, results are expressed as Mean±SD; Two-way ANOVA followed by Bonferroni posttest was used to determine significance. compared with the Con group, *P<0.01) E-F. Protein expression of Myh11, αSma, Mac2 and Cd68 were measured by western-blot. (n=3 per group, results are expressed as Mean±SD; compared with the Con group by repeated-measures ANOVA followed by the Dunnett multiple comparisons test, **P<0.01)

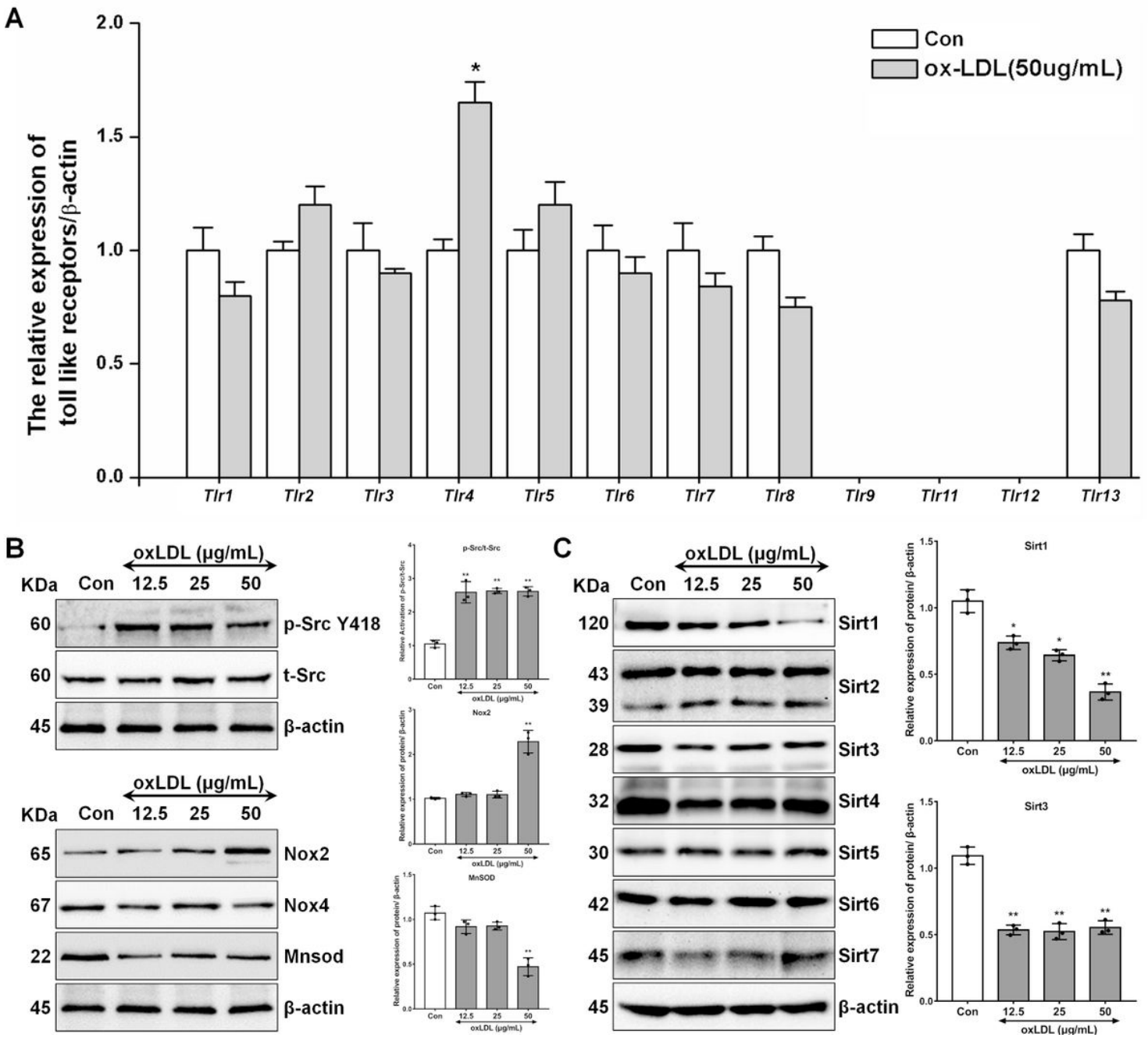

Figure 2

oxLDL regulated expression of toll like receptor family, ROS-related genes and sirtuin family as well as activation of Src. After oxLDL stimulation, the mRNA or protein expression of genes were detected by real-time PCR or western-blot in VSMCs. The phosphorylation of Src were detected using western-blot. Untreated group served as control (Con), and β-actin served as internal reference gene to normalize protein expression. All of the real-time PCR results were calculated by 2-ΔΔCT method, the western-blot results were calculated using grayscale value. A. The mRNA expression of toll like receptor family ranging from Tlr1 to Tlr13. (Two-way ANOVA followed by Bonferroni posttest was used to determine significance. n=3 per group, results are expressed as Mean±SD; compared with the Con group, *P<0.01) B. Upper: The phosphorylation of Src (Tyr-418, Y418) were detected after 1-hour stimulation by different doses (12.5, 25

and 50 μg) of oxLDL in VSMCs. Bottom: The protein expression of ROS generation (Nox2 and Nox4) and elimination (Mnsod) related genes in VSMCs, after stimulating by different doses (12.5, 25 and 50 μg) of oxLDL for 48 hours. C. After incubation with different doses (12.5, 25 and 50 μg) of oxLDL, the protein levels of sirtuin family (Sirt1-7) were measured. (n=3 per group, results are expressed as Mean±SD; compared with the Con group by repeated-measures ANOVA followed by the Dunnett multiple comparisons test, **P<0.01)

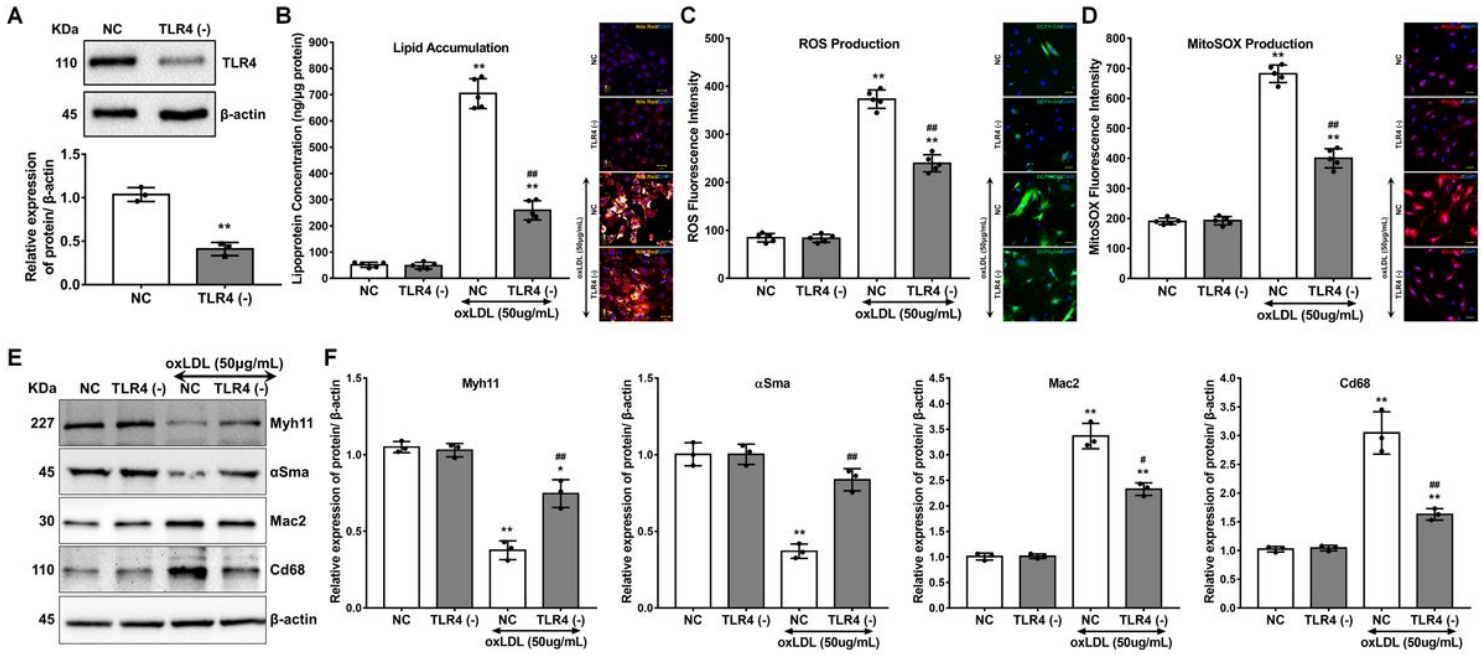

Figure 3

Knockdown of Tlr4 suppressed oxLDL-induced lipid accumulation, ROS and mitochondrial superoxide production, and regulated related genes activation and expression. Tlr4 was knockdown by siRNA transfection within VSMCs. The phosphorylation of Src and other genes expression were detected by western-blot, and β-actin served as internal reference gene to normalize protein expression. All the western-blot results were calculated using grayscale value. A. The Tlr4 –specific [Tlr4(-)] and negative (NC) siRNA were transfected into VSMCs for 72 hours, and the knockdown efficiency was detected. (n=3 per group, results are expressed as Mean±SD; compared with the NC group by Student t test, **P<0.01) B.-C. Tlr4(-) or NC VSMCs were treated with or without oxLDL (50 μg/mL) for 48 hours, B.) lipid accumulation (Nile red stain, Orange), C.) ROS (DCFH-DA, Green) and D.) mitochondrial superoxide (MitoSOX, Red) were measured. (n=5 per group, results are expressed as Mean±SD; Two-way ANOVA followed by Bonferroni posttest was used to determine significance, compared with oxLDL un-treatment, * P<0.05, **P<0.01; compared with NC group, #P<0.05, ##P<0.01.) E. Tlr4(-) or NC were treated with or without oxLDL (50 μg/mL) for 1 hour, the activation of Src (Tyr-418, Y418) had been detected with western-blot. F. – G. Tlr4(-) or NC VSMCs were treated with or without oxLDL (50 μg/mL) for 48 hours, western-blot was conducted to measure oxidative stress-associated genes, VSMCs contractile phenotype markers (Myh11 and αSma) and foam cells markers (Mac2 and Cd68). (n=3 per group, results are expressed as Mean±SD; Two-way ANOVA followed by Bonferroni posttest was used to determine

significance, compared with oxLDL un-treatment, * P<0.05, **P<0.01; compared with NC group, #P<0.05, ##P<0.01.)

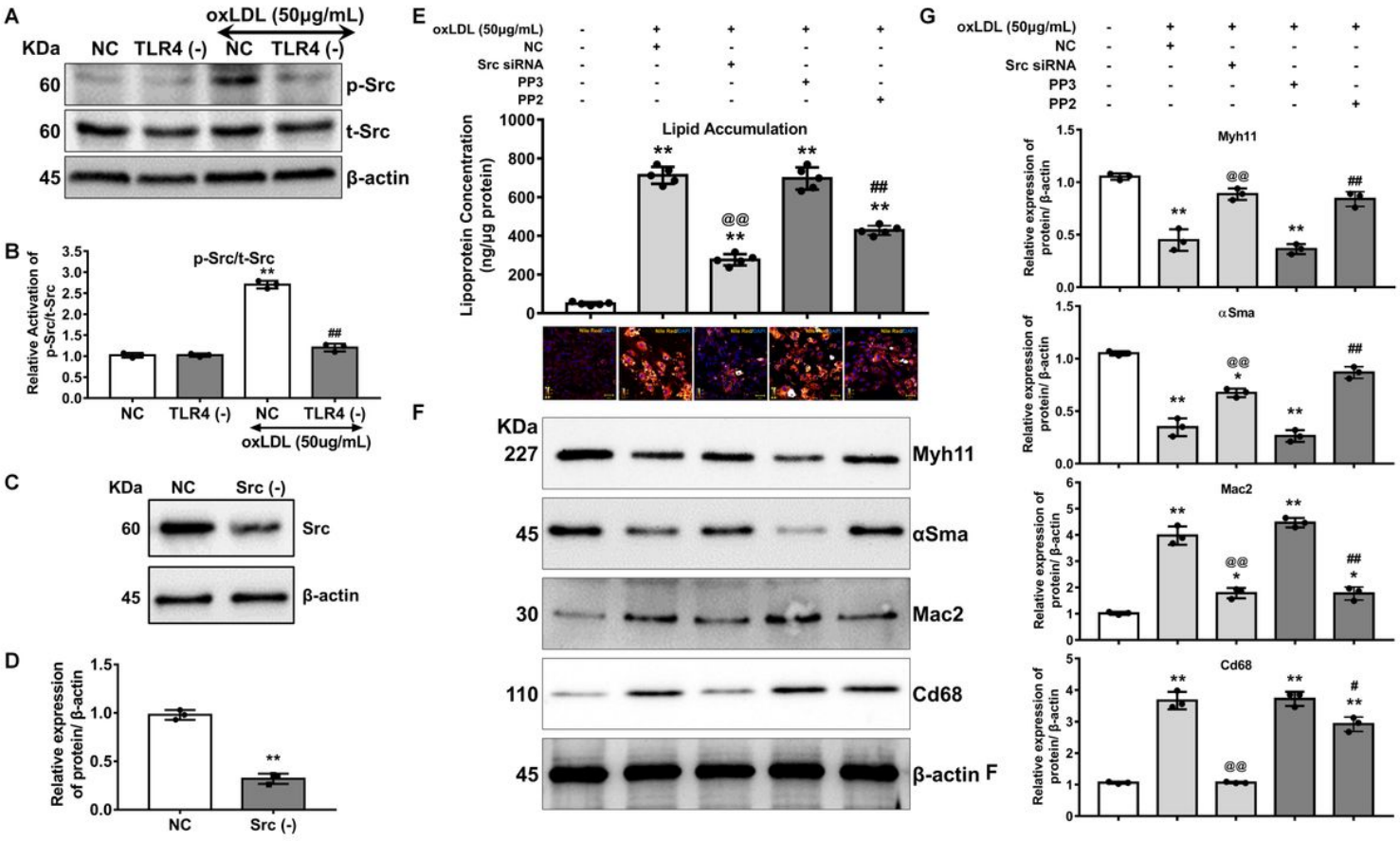

Figure 4

Knockdown or inactivation of Src regulated lipid accumulation and cellular phenotype in VSMCs. Src was knockdown by siRNA transfection within VSMCs. The Src-specific antagonist, PP2, was used to block activation of Src, with PP3 serving as the negative control. The VSMCs were treated with and without 50 μg/mL oxLDL for 48 hours. A. Nile Red (Orange) was used to label the lipid and the concentration of intracellular lipid was measured. (n=5 per group, results are expressed as Mean±SD; 2-way ANOVA followed by the Dunnett multiple comparison procedure and then the Bonferroni posttest was used to determine significance, compared none treatment, **P<0.01; Src siRNA compared with NC group, @@ P<0.01; PP2 compared with PP3, ## P<0.01) B. – C. Western-blot was conducted to measure the VSMCs contractile phenotype markers (Myh11 and αSma) and foam cells markers (Mac2 and Cd68). All the western-blot results were calculated using grayscale value, and β-actin served as internal reference gene to normalize protein expression. (n=3 per group, results are expressed as Mean±SD; 2-way ANOVA followed by the Dunnett multiple comparison procedure and then the Bonferroni posttest was used to determine significance, compared none treatment, **P<0.01; Src siRNA compared with NC group, @@ P<0.01; PP2 compared with PP3, ## P<0.01) D. The Src-specific [Src (-)] and negative (NC) siRNA were respectively transfected into VSMCs for 72 hours, and the knockdown efficiency was detected. (n=3 per group, results are expressed as Mean±SD; compared with the NC group by Student t test, **P<0.01)

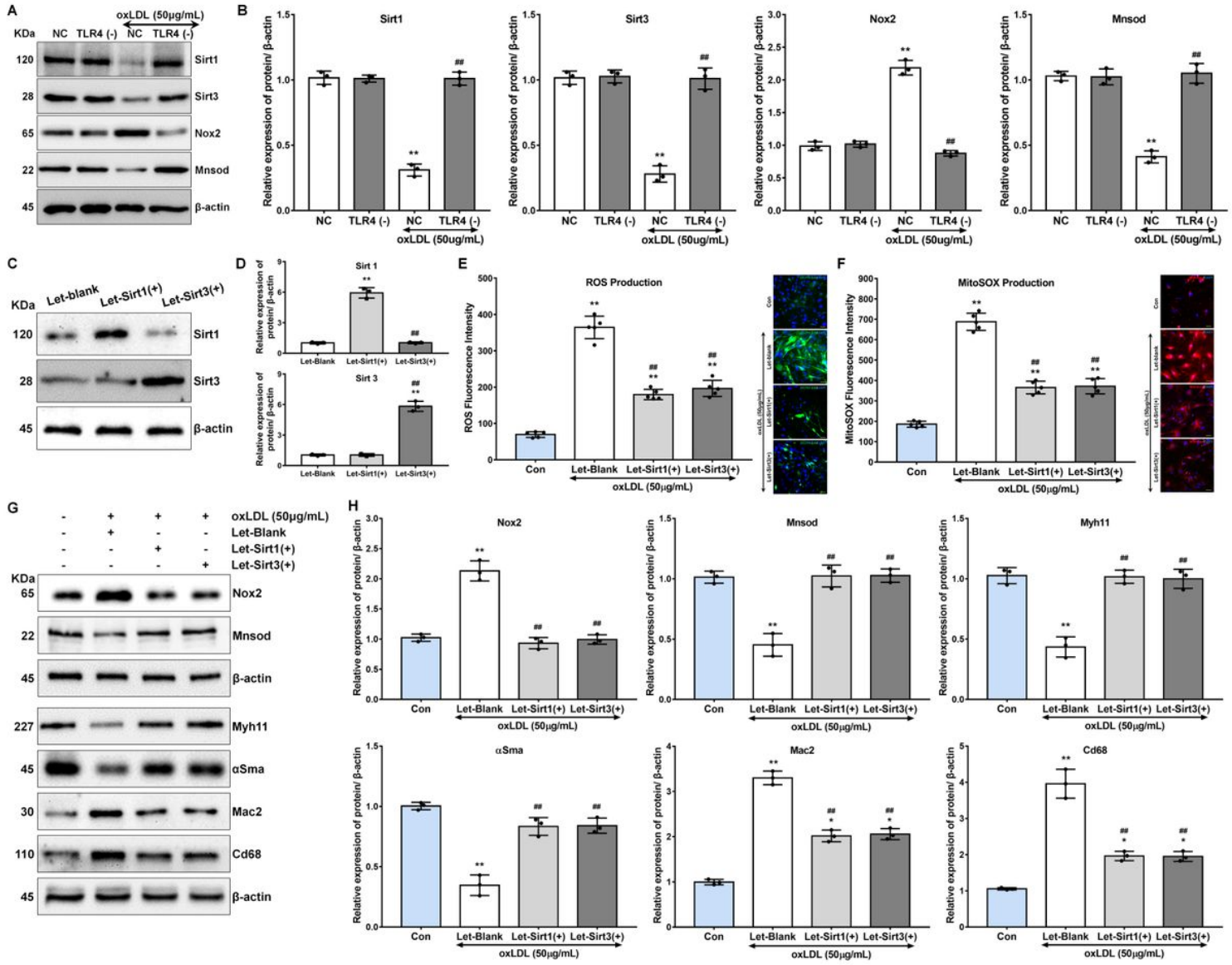

Figure 5

Overexpression of Sirt1 or Sirt3 inhibited oxLDL-induced ROS accumulation and altered cellular phenotype in VSMCs. The recombinant lentivirus of Sirt1 or Sirt3 were infected into VSMCs for Sirt1 and Sirt3 overexpression. The VSMCs were treated with or without 50 μg/mL oxLDL for 48 hours. A. The VSMCs were infected by recombinant lentivirus of Sirt1 [Let-Sirt1(+)] or Sirt3 [Let-Sirt3(+)] respectively for 72 hours, afterwards, the overexpression efficiency was detected. (n=3 per group, results are expressed as Mean±SD; Two-way ANOVA followed by Bonferroni posttest was used to determine significance, compared with the blank lentivirus (Let-Blank) group, **P<0.01; compared with Let-Sirt1(+) group, ##P<0.01) B. ROS (DCFH-DA, Green) and C. mitochondrial superoxide (MitoSOX, Red) was measured. (n=5 per group, results are expressed as Mean±SD; Two-way ANOVA followed by Bonferroni posttest was used to determine significance, compared with none treatment, **P<0.01; compared with Let-Blank group, ##P<0.01.) D. Western-blot was conducted to measure the Nox2 and Mnsod (upper), as well as the VSMCs contractile phenotype markers (Myh11 and αSma) and foam cells markers (Mac2 and Cd68) (bottom). All the western-blot results were calculated using grayscale value, and β-actin served as internal

reference gene to normalize protein expression. (n=3 per group, results are expressed as Mean±SD; Two-way ANOVA followed by Bonferroni posttest was used to determine significance, compared with none treatment, *P<0.05, **P<0.01; compared with Let-Blank group, #P<0.05, ##P<0.01.)

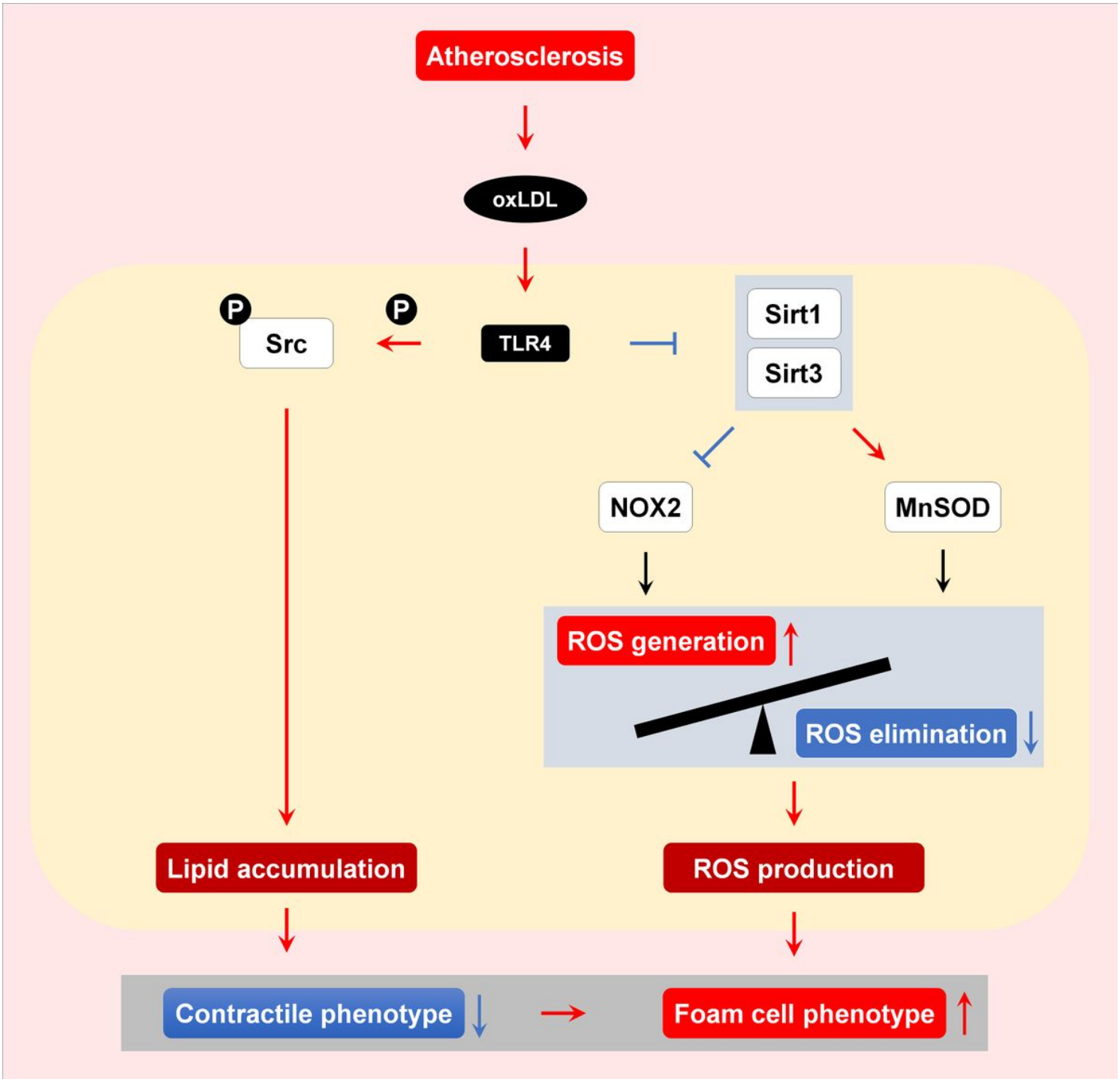

Figure 6

Overall network of Tlr4 in regulating oxLDL induced foam cell formation in VSMCs.